



York, C. B. (2018) Insights Into the Buckling Behaviour of Finite Length Composite Plates with Continuity Over Supports. Stability of Structures XV-th Symposium, Zakopane, Poland, 17-21 Sep 2018.

There may be differences between this version and the published version. You are advised to consult the publisher's version if you wish to cite from it.

<http://eprints.gla.ac.uk/159755/>

Deposited on: 29 March 2018

Enlighten – Research publications by members of the University of Glasgow\_  
<http://eprints.gla.ac.uk>

# Insights into the buckling behaviour of finite length composite plates with continuity over supports.

Christopher B. York

Aerospace Sciences, School of Engineering, University of Glasgow, G12 8QQ, Glasgow, Scotland.

The buckling behaviour of isolated plates has been extensively investigated in the literature for metallic (isotropic) materials across a range of length to width ratios (or aspect ratio,  $a/b$ ), and with a variety of boundary conditions, from simply supported, offering a lower-bound solution, through to clamped, offering an upper-bound solution. The effect of continuity between adjacent plates, i.e., where a plate is continuous over supports, as in aircraft wing and fuselage construction, is less well documented<sup>1</sup>.

Classical garland curves representing compression buckling of an isotropic laminate, continuous over otherwise simple supports, are given in Fig. 1(a). For isotropic material, only the top curve is of relevance, with the runout value, representing the infinitely long plate with buckling factor  $k_{x,\infty} = 4.00$ . Note that whilst compression buckling results for the isolated plate (shown by discrete points) are identical to the continuous plate for isotropic materials, mode interaction due to *Bending-Twisting* coupling (characterised by the magnitude of the lamination parameter  $\xi_{11}$  within the range  $0 < \xi_{11} \leq 0.5$ ) gives rise to very different results. Clamped results are given in Fig. 1(b), in which the continuous plate now degenerates into an isolated plate. Whilst the discrete points representing an isotropic laminate, e.g.  $[-45/90/0/45/0/45/90/45/-45/0/-45/90/-45/90/45/90/0/-45/0/45/0/45/-45/90]_T$ , give identical results there are very significant differences between the continuous and isolated plate cases for *Bending-Twisting* coupled laminates, e.g.  $[45/0/90/-45/90/45_2/0]_S$  with  $\xi_{11} = 0.4$ . The asymptotes representing the infinitely long plate reveal buckling strength reductions of up to 16% below the fully isotropic laminate, or a 10% reduction if practical designs are considered. For clamped edges, the hypothetical buckling strength reduction is up to 14%, or an 8% reduction for the practical designs.

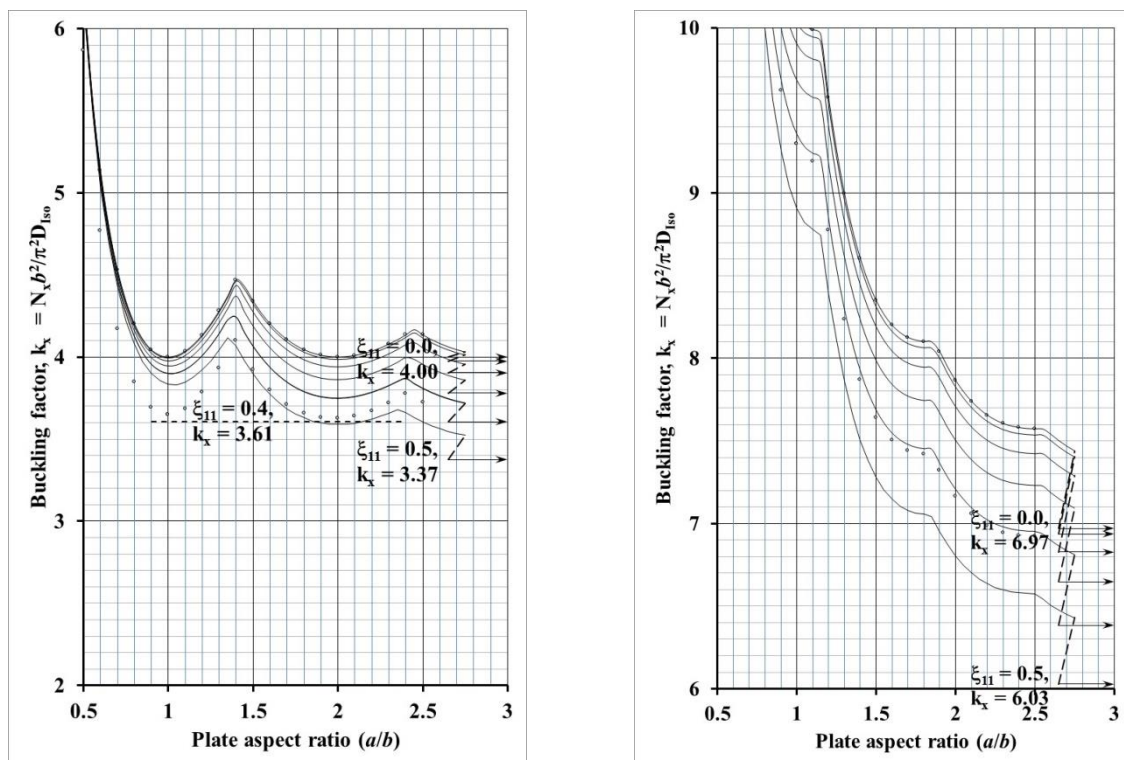


Figure 1 – Compression buckling curves for composite plates, with isotropy in bending ( $\xi_{11} = 0$ ) and subject to increasing magnitude of *Bending-Twisting* coupling ( $\xi_{11} = 0.1, 0.2, \dots, 0.5$ ) with: (a) continuous over otherwise simple supports and: (b) clamped edges. Isolated plate results are illustrated by discrete points.

Laminated composite materials also offer enhancements in buckling performance if correctly designed. However, care must be exercised when the common ‘Balanced and Symmetric’ design rule is adopted, since the resulting *Bending-Twisting* coupling introduced can lead to the substantial reductions in buckling performance demonstrated in Fig. 1.

Buckling solutions are presented as contour maps, representing non-dimensional buckling factors,  $k_x (= N_x b^2 / \pi^2 D_{iso})$  which are superimposed on the lamination parameter design spaces ( $\xi_9, \xi_{10}$ ) for laminated composites with standard ply orientations, i.e., combinations of  $+45^\circ$ ,  $-45^\circ$ ,  $0^\circ$  and  $90^\circ$  plies. For any uncoupled laminate ( $\xi_{11} = 0$ ), the compression buckling load ( $N_x$ ) can be calculated from the closed form solution:

$$N_x = \pi^2 \left[ D_{11} \left[ \frac{m}{a} \right]^2 + 2(D_{12} + 2D_{66}) \frac{1}{b^2} + D_{22} \left[ \frac{1}{b^4} \right] \left[ \frac{a}{m} \right]^2 \right] \quad (1)$$

where elements of the bending stiffness matrix ( $D_{ij}$ ) can be obtained directly for the lamination parameter coordinate ( $\xi_9, \xi_{10}$ ), relating to a practical design, of thickness  $H$ , contained within a laminate database<sup>2</sup>:

$$\begin{aligned} D_{11} &= \{U_1 + \xi_9 U_2 + \xi_{10} U_3\} \times H^3/12 & U_1 &= \{3Q_{11} + 3Q_{22} + 2Q_{12} + 4Q_{66}\}/8 & Q_{11} &= E_1/(1 - \nu_{12}\nu_{21}) \\ D_{12} &= \{U_4 - \xi_9 U_3\} \times H^3/12 & U_2 &= \{Q_{11} - Q_{22}\}/2 & Q_{12} &= \nu_{12}E_2/(1 - \nu_{12}\nu_{21}) \\ D_{22} &= \{U_1 - \xi_9 U_2 + \xi_{10} U_3\} \times H^3/12 & U_3 &= \{Q_{11} + Q_{22} - 2Q_{12} - 4Q_{66}\}/8 & Q_{22} &= E_2/(1 - \nu_{12}\nu_{21}) \\ D_{66} &= \{-\xi_{10} U_3 + U_5\} \times H^3/12 & U_4 &= \{Q_{11} + Q_{22} + 6Q_{12} - 4Q_{66}\}/8 & Q_{66} &= G_{12} \\ & & U_5 &= \{Q_{11} + Q_{22} - 2Q_{12} + 4Q_{66}\}/8 & & \end{aligned} \quad (2)$$

The contour maps of Fig. 2 provide new insights into buckling performance improvements away from the isotropic laminate, with coordinate ( $\xi_9, \xi_{10}$ ) = (0, 0). Changes in buckling mode for finite length plates complicate the contour maps, compared to those for infinitely long plates<sup>2</sup>, since the isolines are now continuous only within discrete regions of the design space. The consideration of shear buckling and/or *Bending-Twisting* coupling further complicates matters, since Eqn. (1) can no longer be used to easily determine the border lines at which modes change.

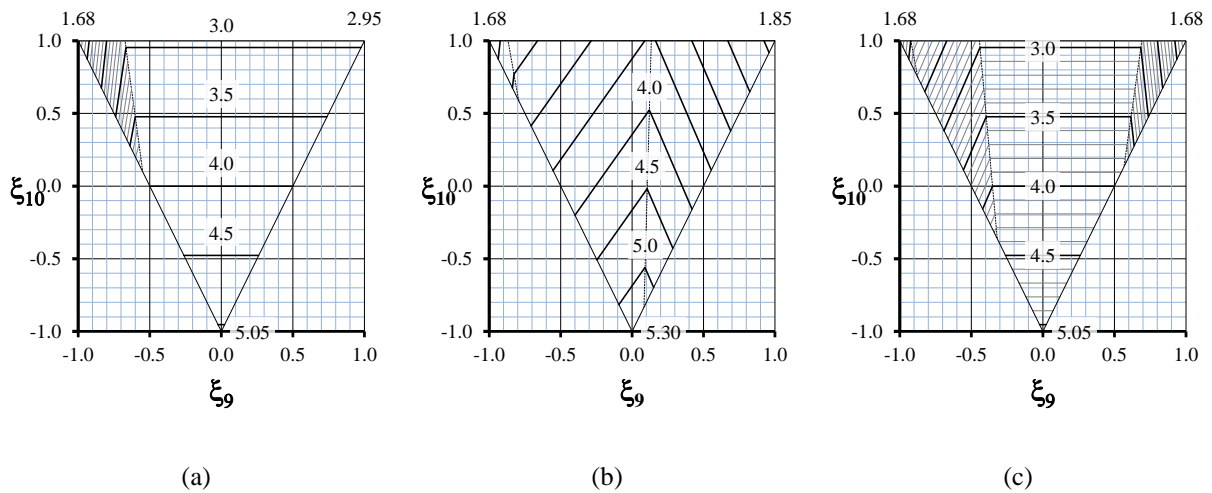


Figure 2 – Lamination parameter design space for compression buckling contours ( $k_x$ ) for uncoupled laminates ( $\xi_{11} = 0$ ) with aspect ratio: (a)  $a/b = 1.0$ ; (b)  $a/b = 1.5$  and: (c)  $a/b = 2.0$ .

## References

1. York, C. (2000) Elastic buckling design curves for isotropic rectangular plates with continuity or elastic edge restraint against rotation. *Aeronautical Journal*, 104(1034), pp. 175-182.
2. York, C.B. (2017) On bending-twisting coupled laminates. *Composite Structures*, 160, pp. 887-900. (doi:10.1016/j.compstruct.2016.10.063)